

Provided for non-commercial research and education use.
Not for reproduction, distribution or commercial use.



This article appeared in a journal published by Elsevier. The attached copy is furnished to the author for internal non-commercial research and education use, including for instruction at the authors institution and sharing with colleagues.

Other uses, including reproduction and distribution, or selling or licensing copies, or posting to personal, institutional or third party websites are prohibited.

In most cases authors are permitted to post their version of the article (e.g. in Word or Tex form) to their personal website or institutional repository. Authors requiring further information regarding Elsevier's archiving and manuscript policies are encouraged to visit:

<http://www.elsevier.com/copyright>



ELSEVIER

available at www.sciencedirect.comwww.elsevier.com/locate/scitotenv

SPME-GCMS study of the natural attenuation of aviation diesel spilled on the perennial ice cover of Lake Fryxell, Antarctica

Caroline M.B. Jaraula^{a,*}, Fabien Kenig^a, Peter T. Doran^a, John C. Priscu^b, Kathleen A. Welch^c

^aDepartment of Earth and Environmental Sciences, University of Illinois at Chicago, 845 W Taylor St., Chicago, Illinois 60607-7059

^bDepartment of Land Resources and Environmental Sciences, Montana State University, Bozeman, MT 59717

^cByrd Polar Research Center, Ohio State University, Columbus, OH 43210-1002

ARTICLE DATA

Article history:

Received 19 March 2008

Accepted 29 July 2008

Available online 18 September 2008

Keywords:

Jet fuel

Naphthalenes

Oil spill

Water washing

Metabolites

SPME-GCMS

ABSTRACT

In January 2003, a helicopter crashed on the 5 m thick perennial ice cover of Lake Fryxell (McMurdo Dry Valleys, East Antarctica), spilling ~730 l of aviation diesel fuel (JP5-AN8 mixture). The molecular composition of the initial fuel was analyzed by solid phase microextraction (SPME) gas chromatography–mass spectrometry (GC–MS), then compared to the composition of the contaminated ice, water, and sediments collected a year after the spill. Evaporation is the major agent of diesel weathering in melt pool waters and in the ice. This process is facilitated by the light non-aqueous phase liquid properties of the aviation diesel and by the net upward movement of the ice as a result of ablation. In contrast, in sediment-bearing ice, biodegradation by both alkane- and aromatic-degraders was the prominent attenuation mechanism. The composition of the diesel contaminant in the ice was also affected by the differential solubility of its constituents, some ice containing water-washed diesel and some ice containing exclusively relatively soluble low molecular weight aromatic hydrocarbons such as alkylbenzene and naphthalene homologues. The extent of evaporation, water washing and biodegradation between sites and at different depths in the ice are evaluated on the basis of molecular ratios and the results of JP5-AN8 diesel evaporation experiment at 4 °C. Immediate spread of the aviation diesel was enhanced where the presence of aeolian sediments induced formations of melt pools. However, in absence of melt pools, slow spreading of the diesel is possible through the porous ice and the ice cover aquifer.

© 2008 Elsevier B.V. All rights reserved.

1. Introduction

The McMurdo Dry Valleys (MCM), which comprise the largest ice-free region of Antarctica, is the coldest and driest desert on our planet and is the site of the MCM long-term ecological research (LTER) program (<http://www.mcmlter.org/>). This polar desert is dominated by microorganisms, the highest forms of organisms being rotifers and nematodes (Roberts et al., 2000). Growth of these organisms occurs during the short summer melt season in the liquid water of the lakes, soils and glacial streams (McKnight et al., 1999; Treonis et al.,

1999), within glaciers (Christner et al., 2005; Foreman et al., 2007), as well as in sediment layers trapped in the perennial ice cover of the lakes (Priscu et al., 1998; Priscu, 1999). Vertebrates and vascular plants are absent (Virginia and Wall, 1999). The cold desert climate, nutrient limitations, and slow-growing biological communities make the MCM ecosystem extremely sensitive to climatic changes and human impact (Cowan and Tow, 2004; Lyons et al., 2006).

The MCM, because of their remote location and severe climate conditions, remained pristine for decades after their discovery in 1903. In the last few decades, increasing

* Corresponding author. Tel.: +1 312 996 7207; fax: +1 312 413 2279.
E-mail address: cjarau1@uic.edu (C.M.B. Jaraula).

exploration, scientific operations, and tourism have affected the MCM, mainly at and around research bases (e.g. Vincent, 1996; Aislabie et al., 2004). Limited tourism started in the valleys in the early 1990s and the MCM-LTER site was established in 1993 (Wharton and Doran, 1999). Helicopter operations related to scientific exploration alone increased by 30% from the early 1970s into the 1990s (Vincent, 1996). Fossil fuel combustion by helicopters in the MCM exceeds that of all other utilities such as stoves, heaters, generators, and all-terrain vehicles (Lyons et al., 2000). During the austral summer of 1995–1996, 106 or 20% of the helicopter landings and take-offs in the McMurdo Sound area occurred at Lake Fryxell in Taylor Valley (Fig. 1A; Wharton and Doran, 1999). Despite the frequency of landings, particulate organic carbon or elemental carbon fluxes derived from helicopters are orders of magnitude lower than the total

active carbon mass in the valleys (Lyons et al., 2000). Most hydrocarbon contaminations in the McMurdo Sound area occurs in landfills, helipads, refueling areas, and from leaks in fuel tanks and fuel lines within McMurdo Station (e.g. Kennicutt et al., 1992; Gore et al., 1999). Relatively high levels of hydrocarbon contamination are also found at research stations in other parts of Antarctica (Saul et al., 2005). A majority of this contamination occurs primarily in soils adjacent to the stations where human activities are focused (Aislabie et al., 2004).

On January 17, 2003, a Bell 212 helicopter crashed on the thick perennial ice cover of Lake Fryxell (Fig. 1). Approximately 730 l of aviation fuel (JP5-AN8) as well as small amounts of hydraulic fluid (MIL 5606), synthetic transmission fluid (Aeroshell 555), and synthetic engine lubricant (Aeroshell 500) were spilled. This accident resulted in the largest documented spill in the MCM. Within four days, an emergency cleanup team from McMurdo Station was dispatched to the crash site. When the approaching winter season forced suspension of the clean-up efforts, it was estimated that no more than 45% of the spilled fluids had been recovered (Alexander and Stockton, 2003). In a review of the potential impacts of research activities in the MCM, Wharton and Doran (1999) concluded that a hazardous spill on the lake ice will have the least impact if cleanup response is immediate. Such action, however, is possible only early in the field season, from September to early November, while the ice is solidly frozen. Spills late in the summer that penetrate the ice cover would be difficult to remove or contain (Jepsen et al., 2006). The crash occurred during a warm period when the lake ice was isothermal near the melting point, and the ice was partly covered by large melt pools, the worst possible scenario for a successful clean-up effort.

Few studies on the impact of accidental hydrocarbon releases in the MCM have been conducted, focusing only on the effects on soil biogeochemistry as most incidents occurred on land (e.g. Lyons et al., 2000; Aislabie et al., 2004). Collectively, these soil-based studies led to the conclusion that hydrocarbon contaminants in this cold desert environment can persist for many years and have profound effects on microbial diversity and geochemistry. However, results of those studies cannot be directly extrapolated to the ice cover, which has significantly different physical, chemical and biological characteristics than soils.

In this report, we compare the initial chemical composition of the fuel spilled on Lake Fryxell ice with that of fuel residue collected a year later in the ice cover. Specifically, we evaluate and compare the effects of biodegradation, evaporation, and water washing on the abundance and composition of the residual aviation diesel fuel. We also discuss the potential for spilled fuel to cross the 5 m ice cover and reach the lake water.

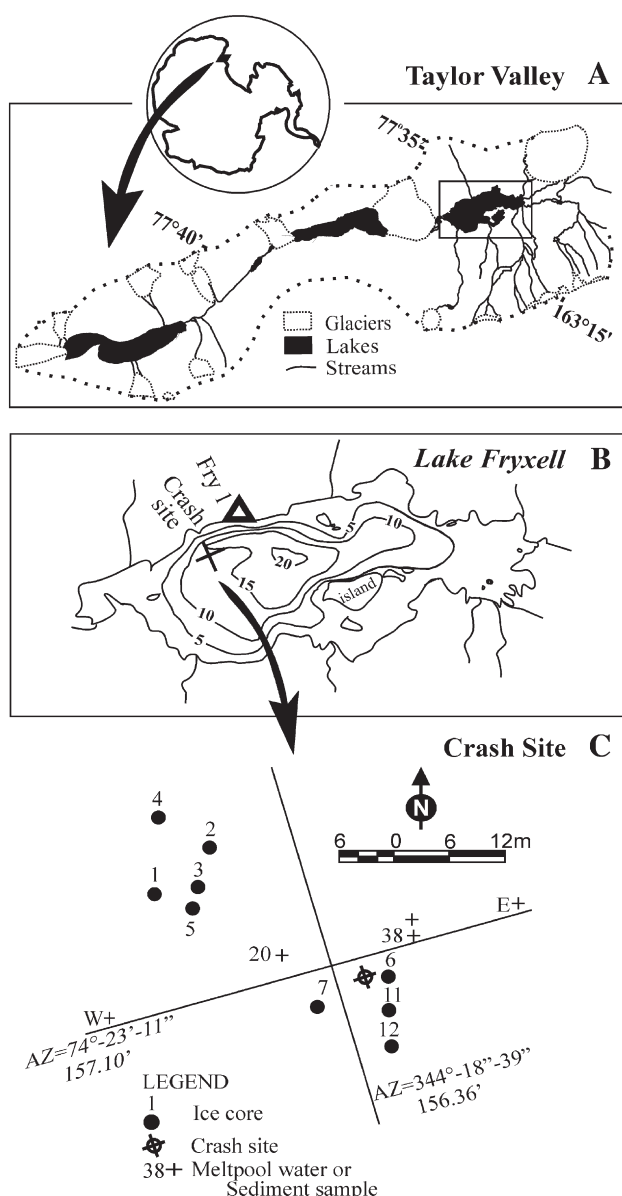


Fig. 1 – (A and B) Helicopter crash site on Lake Fryxell ice cover, Taylor Valley, Antarctica. Locations of meltpool waters, sediments and ice cores collected a year after the crash (C). W = westernmost and E = easternmost samples.

2. Materials and methods

2.1. Study area and ice cover conditions

The helicopter crash site (77°36'41.098" S, 163°06'47.228" E) is located 602 m from the Fryxell Camp benchmark Fry 1 along azimuth 200°50'39" (Fig. 1B; Alexander and Stockton, 2003). At

this site, the ice cover was 5.3 m thick. The average annual ice cover thickness is a balance between 15 to 60 cm y^{-1} of ablation loss at the surface via sublimation, and ~ 30 cm y^{-1} of freezing of lake water at the bottom, generating a net upward movement of the ice cover. Precipitation in the Lake Fryxell basin is minor (<10 cm y^{-1} water equivalent) and almost exclusively as snow (Bromley, 1985). The lake basin typically has 30 melt days (Henderson et al., 1965). Patches of aeolian sand, embedded or covering the ice has a lower heat capacity than the surrounding ice (Adams et al., 1998), and induce the formation of melt pools up to 1.5 m wide on the surface during the austral summer. In the subsurface, the sediments melt into the ice and leave a trail of liquid water in their path (Adams et al., 1998). Some of the sediments collect in pockets and in the summer accumulate at the bottom of cavities in the porous ice. Fritsen and Priscu (1998) identified a layer of sediment at ~ 0.5 m depth in Lake Fryxell and referred to this sediment layer an "aquifer" in the ice as this contains liquid water from November to February. Liquid water volume in the ice cover can be as high as 40% at the peak of summer (Adams et al., 1998).

Coincidentally, prior to the accident, a thermal array was deployed to monitor the temperature of the ice cover near the crash site. During the ten days prior to the crash, maximum daytime temperature was 2–3 °C, considerably warmer than the average summer temperature of -3 °C (Margesin and Schinner, 1999). Above-freezing temperatures resulted in the formation of large melt pools, which exposed subsurface chambers generally 0.2 to 0.5 m beneath the surface with a maximum depth of 1.2 m. These melt pools are mainly located south of the crash site where more sediment had accumulated on the ice (Alexander and Stockton, 2003). The sampling grid (Fig. 1C) separates the northern and southern sectors (Alexander and Stockton, 2003).

Some of the spilled fuel-oil mixture was visible on melt pool surfaces and in subsurface chambers, some of which were accessed with chisels and ice-axes during clean-up operations. On the 18th day after the crash, the contamination was visible to 19 m radius from the crash site (Alexander and Stockton, 2003). Daytime temperatures above freezing lasted until January 23rd, six days after the crash. No temperature data are available from January 23rd until February 6th, when a data logger was installed at the crash site (Alexander and Stockton, 2003). Surface temperatures fluctuated around 0 °C. Temperatures dropped below 0 °C only on the 14th and 16th of February at a depth of 0.25 and 0.50 m, respectively.

2.2. Samples

From December 2003 to January 2004, during the austral summer, approximately a year after the accident, twelve 7.6 cm diameter and 2–4 m long ice cores were collected using a Sipre corer fitted with a two-cycle motor head. In the northwest quadrant of the sampling grid, cores 1 to 5 were collected at sites believed to be uncontaminated, though fuel sheen covered the surfaces of water filling the core holes (Fig. 1C). Cores 6, 11 and 12 were recovered in a summer melt area near the impact site. All of the cores were wrapped in aluminum foil that had been baked at 500 °C for 12 h. The cores were kept frozen at -22 °C until processed at the University of Illinois at Chicago. Seven samples of melt waters were collected from melt pools at the accident site. Separate sediment samples were also collected at sites 20 and 38.

The sediments and water samples were kept at 4 °C until analyzed. Raytheon Polar Services provided a sample of the JP5-AN8 aviation fuel used in McMurdo.

2.3. Core sampling

The upper 70 cm of the cores were logged for brittleness, transparency, presence of bubbles, laminations, and fluorescence under 365 nm ultraviolet (UV) light. Under UV light, JP5-AN8 diesel fuel has a yellow fluorescence, whereas transparent and opaque ice is pink to purple. Subsamples were collected where ice character and UV light fluorescence changes as well as where sediments were present. Subsamples were cut into 1 cm-thick ice chunks by a methanol-cleaned band saw in a -22 °C walk-in freezer. Half of each subsample was archived; the other half thawed at 4 °C in a closed glass jar. All glassware used was baked overnight at 500 °C, and all caps were lined with solvent-cleaned polytetrafluoroethylene.

Fluid in an ice bubble was sampled by manually drilling into the bubble airspace, then collecting with a syringe. Approximately 15 μ l of fluid was recovered.

2.4. Extraction of volatiles

To minimize loss of low molecular weight volatiles, the vapor phases of the melt pool waters and thawed ice water were sampled using solid phase micro-extraction (SPME; Pawliszyn, 1999). A 2000 μ l aliquot of each thawed subsample was pipetted into headspace sampling vials. While the samples were continuously stirred, SPME headspace sampling was performed using a 100 μ m polydimethylsiloxane phase fiber for 10 min at 40 ± 1 °C. For samples overloaded with fuel, a lesser volume of aliquot (10 μ l) was used and diluted with ultrapure water to total 2000 μ l. For the bubble fluid, 0.1 μ l was diluted in 2000 μ l ultra pure water.

2.5. Gas chromatograph–mass spectrometry

A HP-6890 gas chromatogram (GC) coupled to a HP-5973 Mass Selective Detector was used in electron ionization mode at 70 eV with helium as carrier gas. The column was a 30 m long HP-5MS with 0.25 mm I.D. and 0.25 μ m thick film. Mass scan range was 40 to 650 at a rate of three scans per second. Analytes were desorbed from the SPME fiber for 30 s into the injector, which was operated in splitless mode at 220 °C.

Quantification of compounds i -C₁₃ and n -C₁₃ was achieved by integrating peak areas from total ion chromatograms, from which the total abundance of alkanes was also calculated. Total naphthalenes was quantified by calculating the sum of integrated peak areas from mass chromatograms m/z 128, 142, 156 for naphthalene, dimethyl- and ethylnaphthalenes, and trimethylnaphthalenes, respectively.

2.6. Fuel evaporation experiment

Fuel-water mixtures were left uncapped to evaporate in a 4 °C walk-in refrigerator. Six 4000 μ l headspace sampling vials were filled with 1900 μ l ultra pure water and 100 μ l of JP5-AN8 fuel. The vials were sealed after 2, 4, 6, 8, 16 and 21 days.

Composition of the remaining fuel in each vial was analyzed using SPME–GC–MS following the method described above, but with the front inlet operating in 99:1 split mode. Vials were weighed before and after the experiment.

3. Results

3.1. JP5-AN8 fuel mix

The exact ratio of JP-5 to AN8 fuel is most likely in the range 60–70% JP-5 and 40–30% AN8. Specifications of JP-5 are found in MIL-PRF-5624S (1996). This fuel has a high flash point (60 °C) and a freezing point of –46 °C (Edwards, 2007). Specifications for the JP-8 grade aviation kerosene AN8 are contained in MIL-DTL-83133E (1999). This fuel has a flash point of at least 38 °C and a freezing point of –58 °C or lower (DESC, 2005).

The JP5-AN8 aviation diesel consists mainly of compounds with low molecular weights (LMW; 0.864 g/ml at 4 °C; 0.778 g/ml at 25 °C). Short-chain *n*-alkanes (C₇–C₁₆) dominate (~32% of the fuel), whereas *n*-C₁₆ to *n*-C₁₈ are present in trace amounts (Fig. 2A). The most abundant *n*-alkane is *n*-C₁₁. Monomethylalkanes (M) as well as isoprenoids and alkylbenzenes from C₈–C₁₆ are also abundant (Fig. 2B and C). Polycyclic aromatic hydrocarbons (PAHs) including mono-, di- and, ethylmethylated naphthalenes comprise ~4% of the total diesel mix (Fig. 2D). Trimethylnaphthalenes, phenantrene, anthracene and methylanthracene are present in trace amounts.

3.2. Ice cores from “uncontaminated” sites

Cores 1 to 5 were collected northwest of the crash site, in an area designated “uncontaminated” (Fig. 1C). After collection of ice cores 1 to 4, fuel sheen was observed on the water that filled the core holes. The cores generally consisted of opaque granular ice and do not contain any significant layers or patches of sediments (see Supplemental material in Appendix A). Ice cores 2, 4 and 5 did not emit yellow fluorescence under UV light, suggesting absence of diesel contamination. Blank SPME–GC–MS total ion chromatograms from core 2 at 0–2 cm (surface) and 10–11 cm, from core 4 at depths 0–2, 13–14, 39–40, 55–56, and 80–81 cm, core 5 from depths 3–4 and 11–12 cm confirmed the absence of contaminants (see Supplemental material in Appendix A). However, SPME–GC–MS of 67–68 cm from core 4 showed traces of JP5-AN8 hydrocarbons, though it did not fluoresce under UV, indicating that some of the spilled diesel penetrated the uncontaminated area. Bubbles with yellowish fluid at 78 cm in ice core 1 and 13 and 21 cm in ice core 3 emitted fluorescence, again indicating that spilled diesel is present in the “uncontaminated” area.

It can be hypothesized that the fuel sheen on the water filling the core holes may derive from rupture of fuel-filled bubbles during coring but may derive also from contamination of the ice cover aquifer. Lateral transport of contaminants with water within the ice cover, especially within granular ice layers, from more contaminated areas is possible.

3.3. Ice cores in contaminated sites

Ice cores 6 and 12, collected in the contaminated area, were analyzed in detail. For the sake of brevity, only results from

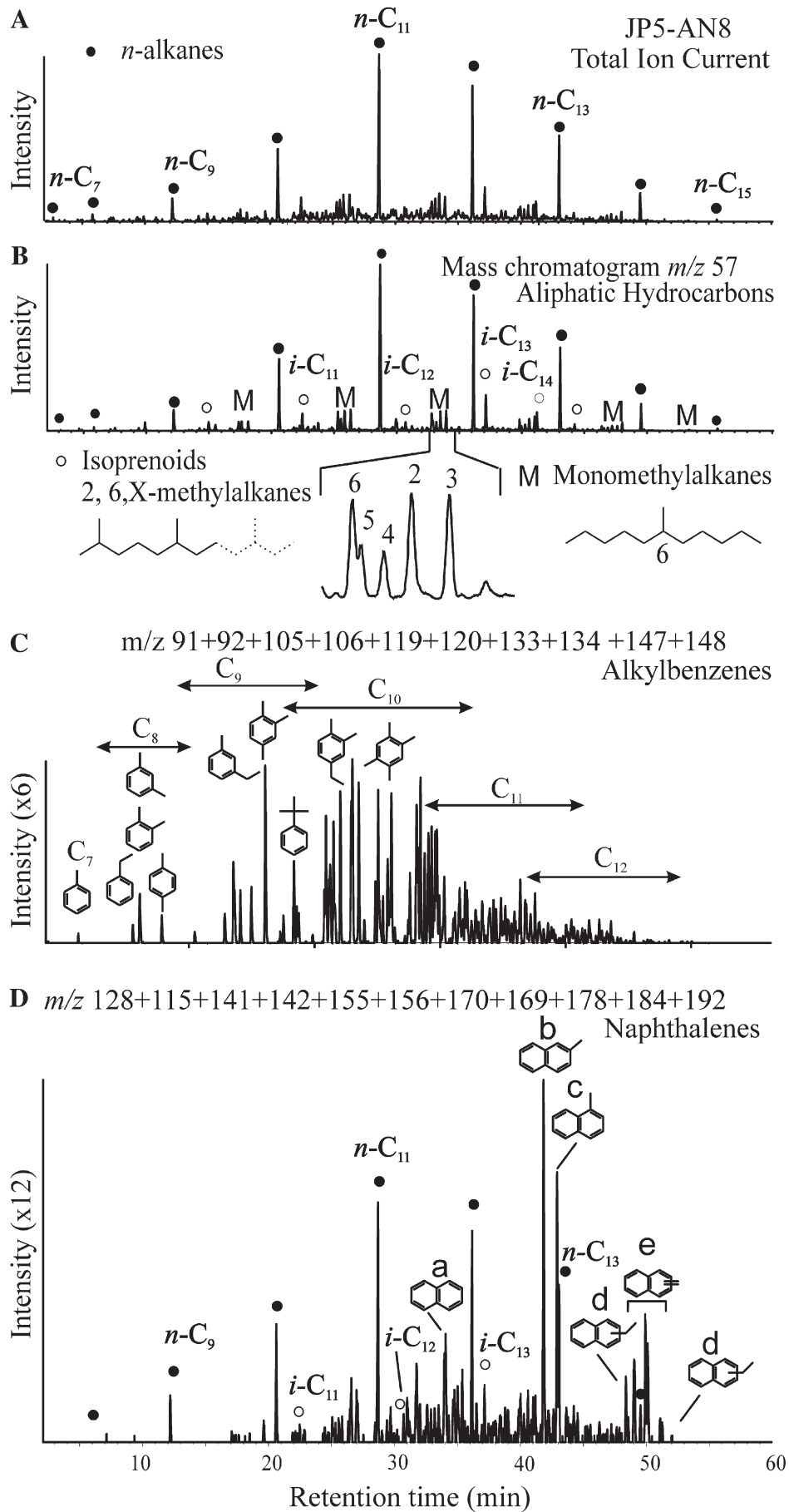
core 12 are described, as this core demonstrate well the various processes involved in fuel compositional changes over time. Description and SPME–GCMS data for ice core 6 are available in the Supplemental material (Appendix A).

The upper 15 cm of ice core 12 comprise two couplets of opaque and transparent ice (Fig. 3). Opaque and granular layers form from rapid freezing or compacted snowfall, whereas transparent ice is formed from slow freezing of pockets of melt waters (Adams et al., 1998). Sparse sediments are present between 5 and 6 cm as well as between 8 and 9 cm. Just above these sediment patches, fluid-filled spherical and inverted teardrop-shaped bubbles emit intense yellow fluorescence under UV light, suggesting abundance of diesel contaminant. The ice between 15 and 30 cm gradually changes from semi-transparent to transparent downward, indicating decreasing rate of freezing from the top to the bottom of the layer. This suggests that the ice between 15 and 30 cm corresponds to the progressive downward freezing of a single melt pool. Between 30 and 48 cm, the core consists of granule to pebble-sized ice chunks with interspersed sediments. Ice chunks with sediments between 45 and 48 cm emit intense yellow fluorescence under UV light, suggesting abundance of diesel contaminant. A prominent sediment layer, between 48 and 53 cm, consisted mainly of angular, fine to granular, buff, white or transparent quartz, and fine to medium black hornblende, other amphibole minerals, and red iron oxide coated angular granules of rock fragments that are all aeolian in origin. The ice from 53–80 cm is transparent and laminated with patches of sediments between 66 and 72 cm. These sediments are similar in composition to those observed between 48 and 53 cm.

SPME–GC–MS results indicate that the surface sample (0–1.5 cm) contained diesel-derived compounds with a mode at *n*-C₁₃ (Fig. 4B, Table 1). A shift in *n*-alkanes distribution mode of the contaminants relative to that of the original fuel (mode at *n*-C₁₁; Fig. 4A) suggests evaporation of low molecular weight compounds. The fluid recovered from an inverted teardrop-shaped bubble at 4 cm has minor compositional differences relative to the JP5-AN8 diesel mixture, suggesting minimal weathering of the diesel as a result of evaporation (Fig. 4C). Aromatic ketones are also present although in low abundance.

The ice between 12 and 13 cm is also contaminated with diesel-derived compounds dominated by *n*-C₁₂ (Fig. 4D), indicating lesser evaporative weathering than for the surface sample. The sample collected between 25 and 26 cm also contains compounds derived from diesel, but dominated by *n*-C₁₃ and with high amounts of naphthalenes relative to *n*-alkanes (Fig. 4E). In this sample, preferential loss of *n*-alkanes compared to branched-alkanes, isoprenoids, and aromatics suggests that biodegradation is the main agent of contaminant weathering as normal alkanes are preferentially degraded relative to branched alkanes, isoprenoids, and cyclic compounds, which in turn are more easily biodegraded than aromatics (e.g. Leahy and Colwell, 1990).

Samples collected between 45 and 46 cm and between 57 and 59 cm contain well resolved PAHs dominated by methylated naphthalenes (Fig. 4F and G). The presence of low molecular weight (LMW) aromatic compounds (120 amu) in sample 45–46 cm precludes evaporation as the only cause of alkane loss. Comparison of the distribution of aromatics in this sample with



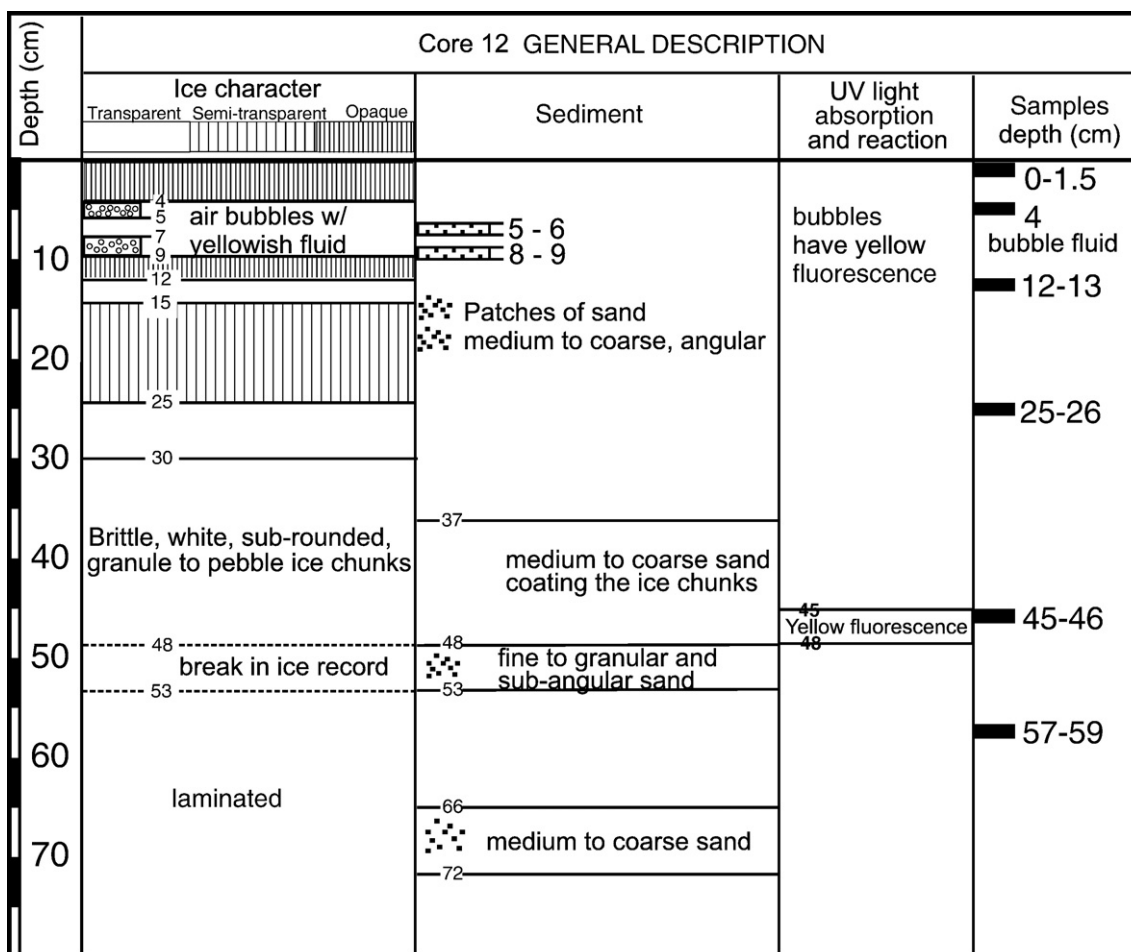


Fig. 3 – Log of ice core 12. Black rectangles indicate samples used for SPME–GCMS analyses.

that observed in the diesel mix (Fig. 5) shows an increase in abundance of LMW relative to high molecular weight (HMW) naphthalenes in the ice sample. Such a change is incompatible with evaporation and biodegradation, which should have affected LMW before HMW compounds (Wang et al., 1998). The well resolved peaks and the absence of an unresolved complex mixture (UCM), typical of biodegraded diesel fuel, excludes biodegradation as a dominant weathering process. Preferential dissolution of LMW PAHs relative to other diesel-derived compounds can account for the exclusive presence of PAHs and their distribution. Zürcher and Thüer (1978) and Bradley and Chapelle (1995) showed that LMW aromatics in petroleum preferentially dissolve in water, resulting in the increased concentration of aromatics in water. Arey et al. (2007) showed that aromatics partition into liquid rather than into air from mass transfer models using vapor pressure and aqueous solubilities. The solubility of PAHs in water generally decreases with increasing molecular weight and varies as a function of alkyl position. This explains why 1-methylnaphthalene (peak c; solubility, 28 mg/L at 25 °C; MacKay et al., 1992) is more abundant than 2-methylnaphthalene (peak b; solubility 24.6 mg/L at 25 °C)

in samples 45–46 and 57–59 cm, but is less abundant than 2-methylnaphthalene in the original fuel (Fig. 5). The increased abundance of naphthalene (peak a; solubility 31 mg/L at 25 °C) relative to both methylnaphthalenes in the ice samples (Fig. 5) can also be explained by preferential dissolution. The same observation can be made for the low abundance of dimethylnaphthalenes (peaks labeled e; least soluble) relative to methylnaphthalenes (more soluble). Therefore, the ice at depths 45–46 cm and 57–59 cm formed from water that was in contact with diesel fuel and in which LMW PAHs were preferentially dissolved and was transported to a subsurface cavity at site 12 where it froze and was sampled. The presence of low molecular weight aromatics in sample 45–46 cm indicates some, but limited, evaporative loss and suggests limited contact between contaminated water and the atmosphere.

The sediment layer between 48 and 50 cm mostly contain aromatics, such as naphthalenes, methyl-, dimethyl- and ethylnaphthalenes (Fig. 4G) but aromatic ketones (such as naphthalenones, indanones, methyl-, dimethyl-, and ethyl-indanones) are also prominent. These aromatic ketones are metabolites formed from biodegradation of aromatic compounds (Langbehn

Fig. 2 – SPME–GCMS of JP-5 and AN8 diesel fuel mixture. (A) Total ion current, (B) n-alkanes, monomethylalkanes, and isoprenoids, (C) alkylbenzenes, and (D) naphthalenes.

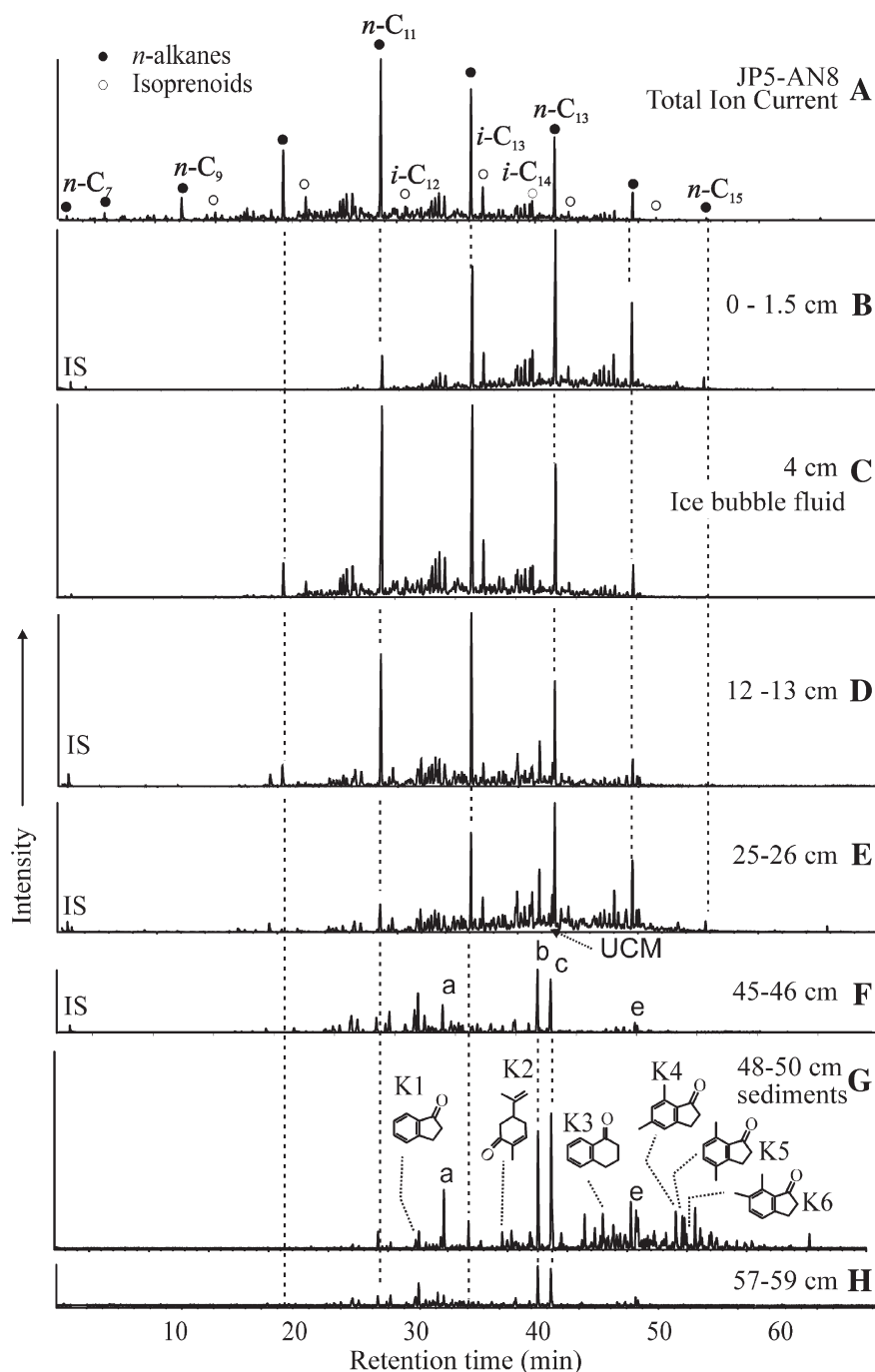


Fig. 4 – SPME-GCMS total ion current of (A) JP5-AN8 diesel mixture, (B–H) ice core 12 samples. Structures of naphthalene homologues a, b, c and d are in Fig. 5A. Core sediments (G) contain biodegradation products of aromatic compounds: K1, 2,3-dihydroindan-1-one, K2, 2-methyl-5-(1-methylethenyl)-2-cyclohexen-1-one, K3, 2,3-dihydro[2H]-naphthalen-1-one, K4, 5,7-dimethylindan-1-one, K5, 4,7-dimethylindan-1-one, K6, 6,7-dimethylindan-1-one. Internal standard (IS) used is trichloroethylene.

and Steinhart, 1995) but have also been considered products of photooxidation (Prince et al., 2003). The contribution of photooxidation to the formation of these ketones cannot be discounted directly, however, we have observed these compounds only in samples associated with sediment layers, where we also observed other effects of biodegradation.

In summary, fuel contained in the surface ice, such as sample 0–1.5 cm is likely to be more frequently exposed to the

atmosphere, enhancing the loss of volatiles and resulting in the strong evaporation signal. More frequent and short-term freeze–thaw cycles produced the alternating layers of sediment in transparent and opaque ice between 4 and 9 cm. Gases exsolved during freezing created bubbles where the fuel was also encapsulated. The fuel trapped into the bubbles is not significantly weathered, though the presence of minor amounts of aromatic ketones suggests biodegradation. It can

Table 1 – Percentage of fuel components and processes affecting the composition of the fuel residue

	AN8	Site 20		Site 38		Core 12 (depths in cm)				
		Water	Sed	Water	Sed	0–1.5	5*	12–13	25–26	45–46
Total alkanes	29	26	33	36	16	35	34	27	20	0
Total naphthalenes	4	11	13	4	15	7	2	7	12	31
Mode	<i>n</i> -C ₁₁	<i>n</i> -C ₁₃	<i>n</i> -C ₁₃	<i>n</i> -C ₁₃	DM-naph	<i>n</i> -C ₁₃	<i>n</i> -C ₁₁	<i>n</i> -C ₁₂	<i>n</i> -C ₁₃	Me-Naph
UCM		Y							Y	
Evaporation		Y	Y	Y		Y		Y	Y	
Biodegradation		Y			Y				Y	
Dissolution							Y			Y

Values are % of total fuel. *Fluid in ice bubble; DM—dimethylnaphthalene; Me—methylnaphthalene; Y—present.

be speculated that this fuel-water inclusion remained fluid for a prolonged period of time and may have formed as an oasis of life in the ice.

In contrast, ice layer between 9 and 30 cm formed from water that froze gradually from the top. The opaque ice layer from 9 to 12 cm froze and quickly insulated the water below and allowed the rate of freezing to decrease as seen from the gradual change in ice character from semi-transparent to transparent between 15 and 30 cm. In samples 12–13 cm and 25–26 cm, the presence of trace amounts of *n*-C₉ (128 amu), a

hydrophobic, insoluble, LMW compound indicates moderate evaporative influence (Fig. 4 D and E). Specifically for sample 12–13 cm, where the mode is at *n*-C₁₂, evaporation was, therefore quickly quenched. With waters from 25–26 cm freezing much slower than the rest of the unit, biodegradation may have persisted longer, resulting in the significant alkane depletion observed (Fig. 4E).

The distribution and abundance of diesel contaminants between 25 and 26 cm as well as between 12 and 13 cm suggest loss of LMW contaminants via biodegradation and evaporation, without any suggestion of selective dissolution of diesel compounds. Thus, the ice samples 25–26 cm and 12–13 cm are derived from a pool of water different from the ice samples 45–46 cm and 57–59 cm, which contain selectively dissolved compounds.

3.4. Meltpool water and sediment

Samples of meltpool water collected from the easternmost and westernmost areas of the crash site (E and W, respectively in Fig. 1B and C) have no detectable fuel contamination with SPME-GC-MS (Fig. 6B and C). In contrast, meltpool water and sediment samples collected closer to the crash site (locations 20 and 38) contained abundant JP5-AN8 residues (Table 1, Fig. 6D–G).

The large amount of diesel fuel contaminant in the water sample from site 20 imposed dilution of 10 μ l of water sample in 1990 μ l of ultra pure water for SPME-GC-MS analysis. Volatiles in meltpool water of site 20 contain *n*-alkanes, with a mode at *n*-C₁₃, indicating significant loss of low molecular weight components by evaporation (Fig. 6D). Branched alkanes and isoprenoids are also abundant, whereas naphthalenes are present in trace amounts.

Sediments in the meltpool at site 20 also contain JP5-AN8 hydrocarbons, with *n*-C₁₃ as the mode (Fig. 6E). As observed in the original fuel mixture, naphthalenes are in low abundance. Branched alkanes and isoprenoids are also present, although less prominent than in the water sample (Fig. 6D). The high isoprenoid to alkane ratio in the water sample relative to the sediment sample suggests a stronger effect of evaporative attenuation in the water sample.

At site 38, the meltpool water is dominated by alkanes with *n*-C₁₃ and *n*-C₁₄ similarly abundant (Fig. 6F). Branched alkanes and isoprenoids are also prominent. This hydrocarbon distribution suggests evaporative loss similar to that observed for the surface sample of nearby core 6 (see Appendix A).

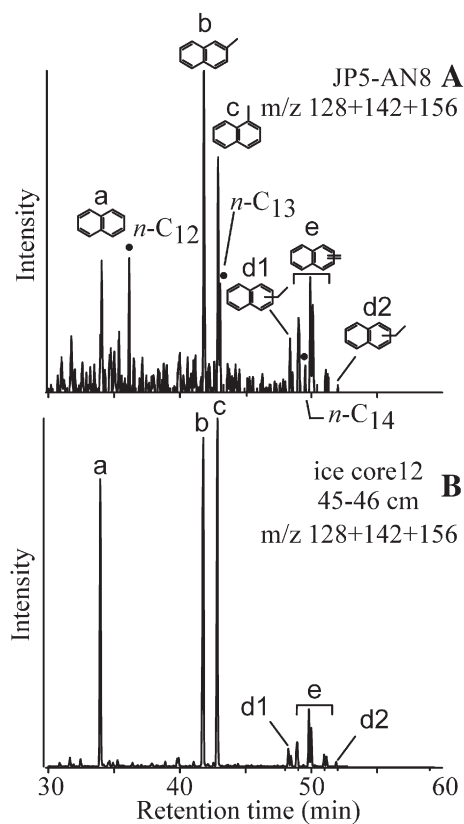


Fig. 5 – Summed mass chromatogram *m/z* 128 + 142 + 156 showing the relative abundance of naphthalenes in (A) JP5-AN8 diesel mixture and (B) in ice core 12, 45–46 cm. a. naphthalene. b. 2-methylnaphthalene, c. 1-methylnaphthalene, d1 and d2. ethylnaphthalenes, e. dimethylnaphthalenes.

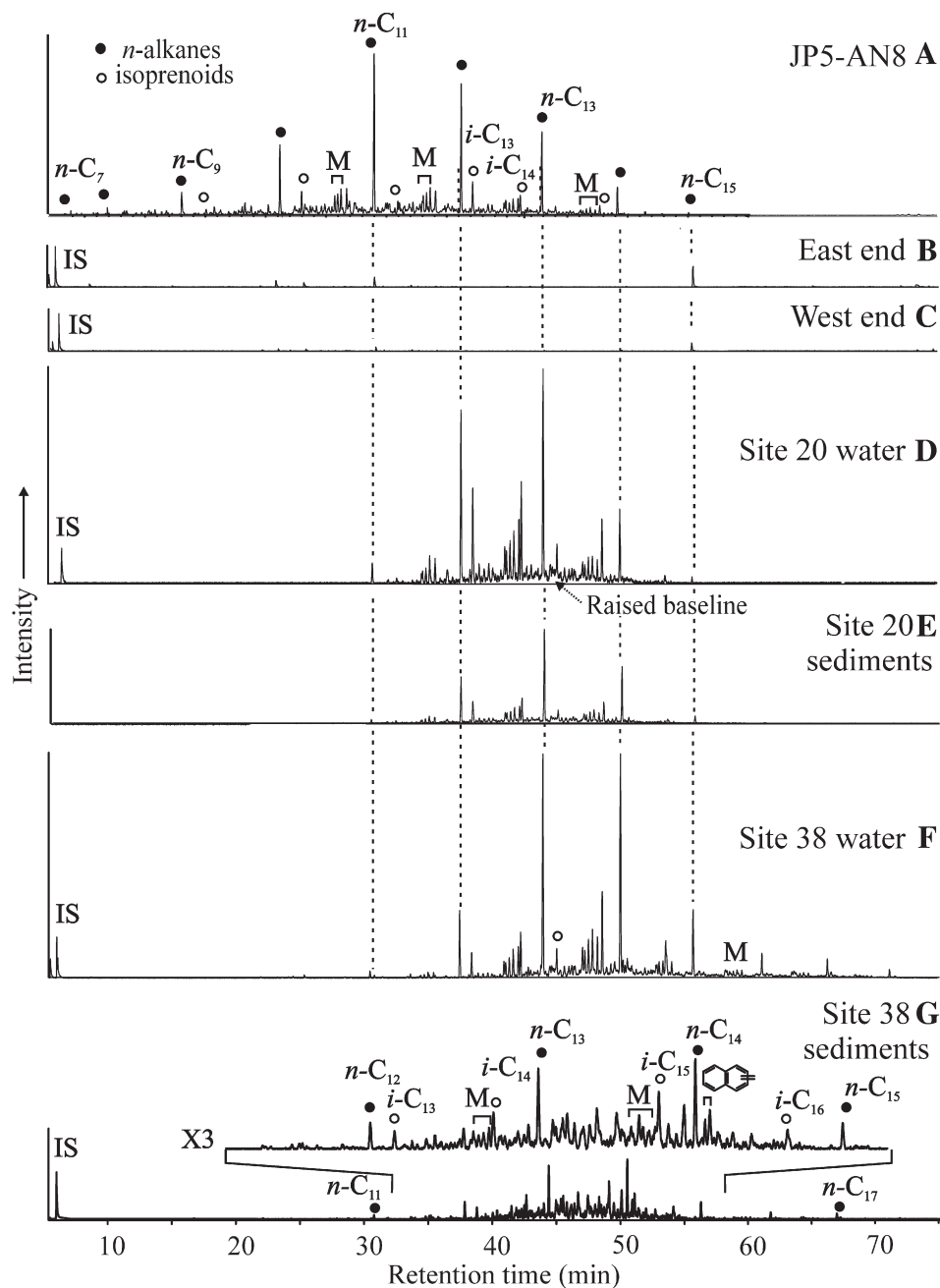


Fig. 6 – SPME-GCMS total ion current of (A) JP5-AN8 diesel mixture and for (B–D) meltpool waters and sediments. Internal Standard (IS) used is trichloroethylene.

The sediment sample from site 38 (Fig. 6G) has much less total fuel hydrocarbons than in the water at site 38. Total *n*-alkanes and total naphthalenes have equal abundances (Table 1), suggesting biodegradation of the diesel. Overall, dimethylnaphthalenes are the most abundant compounds, followed by *n*-C₁₄. Evaporative loss seems equivalent in both water and sediment samples.

3.5. Fuel evaporation experiment

As the aviation diesel evaporated, combined weights of the water and fuel for each sampling day decreased. By the sixth day, the weight loss was about 80 mg, or ~10% of the initial fuel

weight. The rate of loss was highest during the first day at 0.7 mg h⁻¹, then decreased to 0.3 mg h⁻¹ on the eighth day. After the eighth day, weight losses were so small that they could not be monitored accurately.

The total ion chromatogram shows a change in the mode from *n*-C₁₁ in the original fuel to *n*-C₁₁ and *n*-C₁₂ by the fourth day, to *n*-C₁₂ by the sixth day, and to *n*-C₁₃ by the sixteenth day. Both *n*-C₁₃ and *i*-C₁₃ increase in percentage of the total fuel residue with time, as LMW volatile compounds are evaporated first. However, the ratio of *i*-C₁₃ over *n*-C₁₃ in the evaporating fuel progressively decreases as *i*-C₁₃ is more volatile than *n*-C₁₃. The *i*-C₁₃/*n*-C₁₃ ratio varied linearly with time during the evaporation experiment ($r^2=0.99$; $n=6$;

see Supplementary material). The abundance of total naphthalene (sum of naphthalene, methyl-naphthalenes and dimethyl-naphthalenes), and total alkane was also monitored. Both groups of compounds increase in percentage of the total fuel residue but the total naphthalene over total alkane ratio also increases with progressive evaporation ($r^2=0.89$; $n=6$; see Supplementary material).

4. Discussion

4.1. Evaporation

Evaporation is a major process in the weathering of the aviation diesel spilled on the ice cover of Lake Fryxell as all samples, including the fluid trapped in ice bubble, show evaporative losses. Evaporation may have occurred as soon as the fuel came in contact with the atmosphere during the accident. Further evaporation of the diesel mixture continued whenever the contaminants were exposed to the atmosphere. In ice cores, evaporation of diesel contaminants is more intense in surface than in deeper layers, as the former is more often subjected to freeze–thaw cycles than the latter (Fig. 4). The light non-aqueous phase liquid (LNAPL) behavior, the dominance of LMW compounds, and the high volatility of spilled aviation diesel favor evaporation.

4.2. Biodegradation

Biodegradation is another major attenuation process in the ice cover, but the effects of this process were exclusively observed in ice containing sediments (Figs. 4G and 6G). In the ice cover, an ecologically and physiologically complex microbial consortium develops from the relatively nutrient- and carbon-enriched mixture of sediment and water (Priscu et al., 1998). Such microbial assemblages were not observed in sediment-free ice layers. The sediments are transported to the ice through aeolian processes from soil and stream habitats and provide the inoculums for in-ice habitat (Fritsen and Priscu, 1998). Viable microbial assemblages are capable of photosynthesis, nitrogen fixation, and decomposition. Filamentous cyanobacterial genus *Phormidium*, nitrogen-fixing genus *Nostoc*, and diatom algae were identified (Priscu et al., 1998). The microbial assemblage must have shifted to organisms more capable of degrading diesel as observed in contaminated Antarctic soils (Saul et al., 2005).

4.3. Evaporation vs. biodegradation

Estimating the relative effect of evaporation and biodegradation on natural attenuation using field samples can be difficult. Snape et al. (2005) developed fuel evaporation models to quantitatively differentiate the effects of evaporation from those of biodegradation of diesel in cold environments (4 °C). Their experiments were based on a diesel fuel, Special Antarctic Blend, which is most often used and spilled at Casey Station (Australian Antarctic base). This diesel, with a n -alkane mode at n -C₁₂, is enriched in HMW compounds compared with the JP5-AN8 mixture studied in this report. Most of the ratios of Snape et al. (2005) include i -C₁₆

concentration. This compound is either unresolved or absent from our SPME-GCMS chromatograms, as JP5-AN8 is a lighter diesel than the Special Antarctic Blend. Thus, for this study, we use the ratio i -C₁₃/ n -C₁₃ of the sample (S) divided by the same ratio in the original diesel (D) mixture as an indicator of evaporation $(i\text{-C}_{13}/n\text{-C}_{13})_S/(i\text{-C}_{13}/n\text{-C}_{13})_D$.

n -C₁₁ or n -C₁₂ could not be used as these compounds are often in low abundance in the chromatographic traces of field samples. As i -C₁₃ evaporates more easily than n -C₁₃, a ratio value of less than 1 indicates evaporation.

Concordant with qualitative observations, quantitative estimate of evaporations using the $(i\text{-C}_{13}/n\text{-C}_{13})_S/(i\text{-C}_{13}/n\text{-C}_{13})_D$ show that contaminants in all samples are primarily affected by evaporation (Fig. 7). Consistent with qualitative observations based on n -alkane mode, the contaminants in the surface sample of core 12 (0–1.5 cm) were affected by evaporation more than contaminants located deeper in the core. Diesel contaminants in meltpool waters are more affected by evaporation than their corresponding sediments as the sediments are shielded from the atmosphere by overlaying waters (see samples for sites 20 and 38 in Fig. 7). It is noteworthy that the contaminants in the bubble fluid at ice core 12 4 cm is the least evaporated of all samples, as observed qualitatively.

As a proxy for the extent of biodegradation we calculated a ratio of the concentrations of total naphthalene (T_{naph}) over the concentration of total alkanes (T_{alk}). As biodegradation intensifies, the ratio increases because alkanes are more easily biodegraded than naphthalenes. However, evaporation affects abundances of both naphthalenes and alkanes and the ratio $T_{\text{naph}}/T_{\text{alk}}$ as a result of their differential response to evaporation and their difference in initial abundance. To circumvent that caveat, an evaporation curve based on an evaporation experiment at 4 °C was plotted on a $(i\text{-C}_{13}/n\text{-C}_{13})_S/(i\text{-C}_{13}/n\text{-C}_{13})_D$ versus $T_{\text{naph}}/T_{\text{alk}}$ diagram (Fig. 7). Field samples falling to the right of the evaporation curve were affected by biodegradation. For example, fuel residues in the sediments of meltpool site 38 are more intensely biodegraded than the meltpool diesel in the ice of Core 12 between 25 and 26 cm.

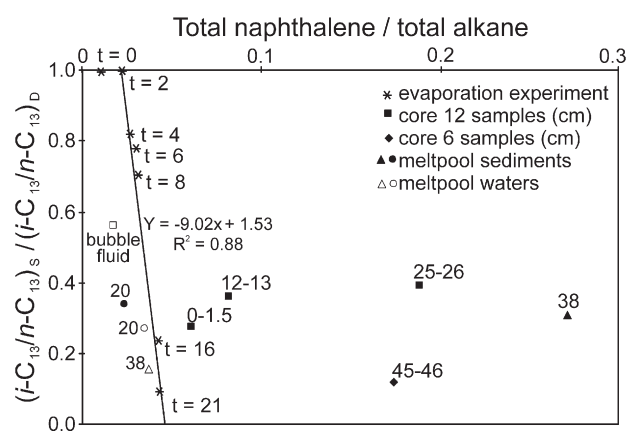


Fig. 7 – $T_{\text{naph}}/T_{\text{alk}}$ versus $(i\text{-C}_{13}/n\text{-C}_{13})_S/(i\text{-C}_{13}/n\text{-C}_{13})_D$ showing the relative strengths of evaporation versus biodegradation in sediments, meltpool waters and ice core subsamples. The evaporation curve is a linear regression.

4.4. Water washing

Samples located to the left of the evaporation curve have lost naphthalenes preferentially to alkanes. The only process we have identified able to explain these data is loss of naphthalenes by preferential dissolution of these compounds in water (water washing). Indeed, we have analyzed ice core samples containing only aromatic compounds that were preferentially dissolved (washed-out) from the diesel contaminants (core 12 45–46 cm and 57–59 cm; Fig. 4F and G) and could not be plotted in Fig. 7 as they do not contain any *n*-alkanes. At site 20, slight variation in $T_{\text{naph}}/T_{\text{alk}}$ indicates higher water washing in the meltpool sediments than in the water. It is noteworthy that the diesel trapped in the bubble of core 12 at 4 cm is partly water-washed, a process that we could not detect qualitatively from the chromatographic trace.

It is important to note that water washing is not a natural attenuation process, as the dissolved compounds are not eliminated from the environment. On the contrary, the preferential transfer of aromatics in water, away from sediments where biodegradation preferentially takes place, will probably prevent or at least slow down the natural attenuation of these compounds.

4.5. Lateral and vertical transport of contaminants

Wharton and Doran (1999) noted that the initial conditions of the ice cover are of paramount importance when considering clean-up efforts, as hard ice of the early summer is easier to clean than the porous and wet ice of the melt season. Early in the season, the solidly frozen ice cover will be mostly impermeable, preventing penetration of contaminants into the ice cover. The

contaminants will more likely spread on the ice surface, enhancing attenuation via evaporation, and most probably sorb on windblown surface sediments. As the summer melt season advances, the porosity, permeability, and water content of the ice cover increases with formation of melt pools, subsurface chambers and channels (Adams et al., 1998; Fritsen and Priscu, 1998), as observed in the southern quadrant of the crash area. Spilled fluids are then able to penetrate the ice cover, and transport of contaminants is more widespread both laterally and vertically. However, the presence of sediments is not merely detrimental as biodegradation was observed only in ice containing sediments. Porous ice north of the crash site, however, allowed the transport of contaminants to previously “uncontaminated” sites within a year after the crash, as indicated by oil films at the surface of water filling the core hole (e.g. ice core 4, 36 m from the crash site).

Transported waters into uncontaminated sites may also have enhanced LMW PAH content as a result of water washing (Fig. 4F and H). Higher molecular weight PAHs such as dimethyl-, ethyl-, and trimethyl naphthalenes were observed unaffected by biodegradation after 1 year. Their solubility will allow future remobilization if in contact with water. As a result, these compounds will likely affect a wider area with time. These compounds, particularly dimethyl- and ethyl-naphthalene may be used as tracers to monitor the spread of residual fuel contamination as they are not occurring naturally in the ice cover.

Ice cover ablation at the surface and the accretion of ice at the bottom yield a net upward movement of the ice cover without reducing its thickness (Fig. 8A). This upward flux of ice will help prevent the contaminants from reaching the lake water if the contaminants do not move downward faster than 60 cm y^{-1} , the

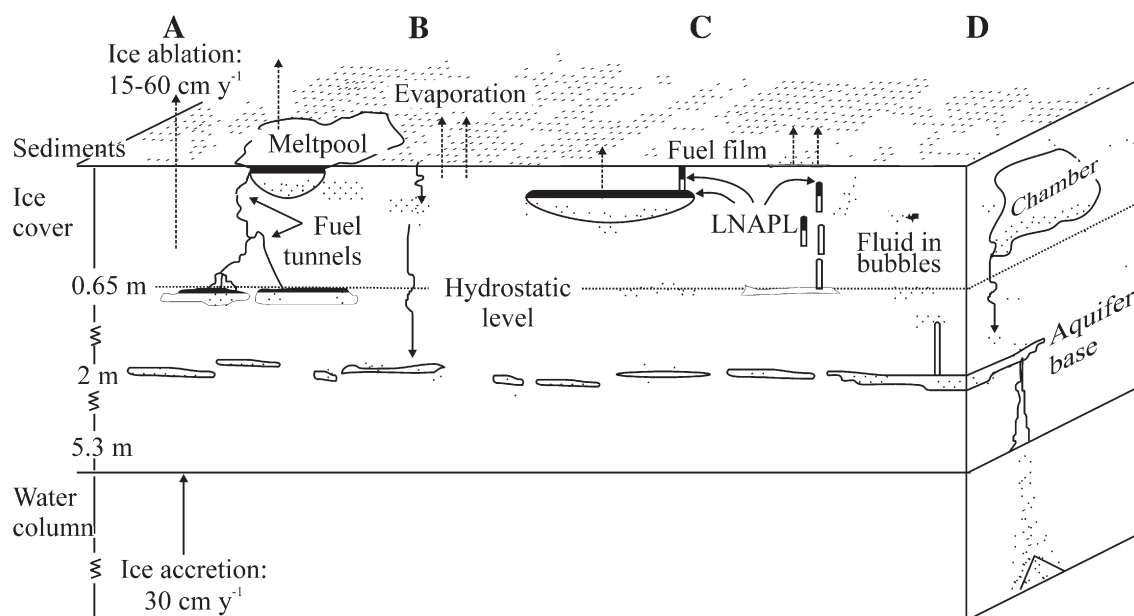


Fig. 8—Dynamics in the Lake Fryxell ice cover that affect the natural attenuation of contaminating fluids. (A) Ablation loss at the surface and accretion of ice at the bottom generates a net upward movement of 30 cm y^{-1} . (B) Light diesel components evaporate from ice surface and melt pools. Lower heat capacity of fuel and sediments induce melting and results to “tunneling” deeper into the ice (Jepsen et al., 2006). (C) Pools of water separate light non-aqueous phase liquids, LNAPLs, making them susceptible for evaporation. LNAPLs may also rise in ice straws and eventually evaporate. (D) Fractions of aromatics that are dissolved are re-frozen in subsurface chambers. Some ice cracks connect the “aquifer” to the lake water.

maximum ablation rate calculated (Henderson et al., 1965). Jepsen et al. (2006), however, showed experimentally that, at temperatures close to ice melting, aviation diesel JP-8 propagates along ice crystal boundaries at velocities up to 1.6 m h^{-1} ("fuel tunneling" Fig. 8B). The extent of vertical fuel tunneling in the field, however, is difficult to predict as tortuosity and branching of the fuel tunnels depend on the concentration of impurities and temperature variations in the ice.

Windblown sediments trapped in the ice cover that are $<1 \text{ cm}$ in diameter are able to melt their way into the ice (Hendy, 2000). Pockets of sediments accumulate up to 2 m in the ice and create an aquifer in the summer (Priscu and Foreman, in press; Fig. 8B). Compared to the heat capacity of ice or water ($0.502 \text{ cal g}^{-1}\text{.}^{\circ}\text{C}^{-1}$), black basaltic sediment ($0.201 \text{ cal g}^{-1}\text{.}^{\circ}\text{C}^{-1}$) and diesel ($0.014 \text{ cal g}^{-1}\text{.}^{\circ}\text{C}^{-1}$) have much lower heat capacities. The presence of diesel contamination will also favor melting of the surrounding ice. We have observed diesel sorbed onto sediment grains, in ice cores and melt pools (sites 20 and 38). Thus, the diesel residues sorbed on the sediment grains will favor the formation of water and sediment pockets and increase the potential for biodegradation as microbial processes are triggered by the presence of liquid water in the summer.

The diesel contaminant, if not associated with sediments, will behave as LNAPLs. The low heat capacity of the diesel can result in the melt of the surrounding ice and the LNAPLs can progressively melt their way to the surface of the ice cover (Fig. 8C). Such a process is commonly observed for pieces of microbial mats, which were incorporated at the bottom of the ice and observed to travel across the ice cover (Parker et al., 1982). When reaching the surface of the ice cover, the contaminants may be further attenuated by evaporation or may associate with sediments and be biodegraded.

The dissolved fraction of the diesel contamination, mostly including the LMW PAHs, will be mobile during the melt season. In all ice samples containing the dissolved portion of water-washed diesel (Fig. 4F and H), we have not observed any of the potential effects of biodegradation. Thus, these compounds are likely to be persistent and natural attenuation will depend on evaporation only.

As sediments can melt their way to a depth of approximately 2 m in the ice cover, where the ice aquifer occurs, it can be speculated that diesel contamination will easily reach that level over time (Fig. 8D). Remobilization of soluble aromatic compounds in the aquifer and the existence of discrete conduits, such as ice cracks, that connect the ice aquifer to the lake water (Hendy et al., 2000) may result in the transfer of soluble aromatic contaminants (e.g. naphthalenes) and sediments coated with fuel into the lake water (Fig. 8D).

Fortunately, the conjugated effects of evaporation and biodegradation, as well as the permanent upward movement of the ice cover will limit to a minimum the amount of diesel components able to reach Lake Fryxell water body.

5. Conclusions

With the helicopter crash occurring late in the summer, the situation was highly unfavorable as above freezing temperatures days prior to and after the crash induced the formation of melt pools and subsurface chambers. Spreading of the

contaminants from the crash site occurred both horizontally and vertically. The extent of horizontal spread is controlled by the volume of pore spaces and network of channels in the ice, which are well developed in the southern quadrants. Diesel contaminated waters also spread into the northern sector, which have porous ice.

A year after the crash, a significant amount of spilled fluid remained in the Lake Fryxell ice cover, particularly south of the crash site. JP5-AN8 is attenuated naturally mainly by evaporation, especially on the ice surface and in melt pool waters. Spilled fluids evaporate at decreased rates during the long Austral winter while confined in the ice cover. Further natural attenuation occurred through biodegradation, especially in sediment-bearing ice layers in which biological activity was previously detected. Alkane-degraders in the ice play as prominent a role in weathering hydrocarbons as they do in the soils, although the rates are much slower.

Acknowledgments

This project was supported by the Office of Polar Program of the National Science Foundation (Antarctic Biology and Medicine SGER 0346316) and by a fellowship grant from the University of Illinois at Chicago Institute of Environmental Science and Policy. Kelvin Rodolfo is acknowledged for his edits on the manuscript. We thank Apostolis Sambanis, Marcus Muccianti, Timothy Chung, and Jeffrey Fitzgibbons who helped in the laboratory.

Appendix A. Supplementary data

Supplementary data associated with this article can be found, in the online version, at doi:10.1016/j.scitotenv.2008.07.064.

REFERENCES

- Adams EE, Priscu JC, Fritsen CH, Smith SR, Brackman SL. Permanent ice covers of the McMurdo dry valley lakes, Antarctica: bubble formation and metamorphism. In: Priscu JC, editor. Ecosystem dynamics in a polar desert: the McMurdo dry valleys, Antarctica. Am. Geophys. Washington DC: Union; 1998. p. 281–95.
- Aislabie J, Balks MR, Foght JM, Waterhouse EJ. Hydrocarbon spills on Antarctic soils: effects and management. Environ Sci Technol 2004;38:1265–74.
- Alexander SP, Stockton WL. Lake Fryxell 79U crash site: initial hydrocarbon monitoring program. Raytheon Technical Services Company; 2003. 44 pp.
- Arey JS, Nelson RK, Plata DL, Reddy CM. Disentangling oil weathering using GCxGC. 2. Mass transfer calculations, Environ Sci Technol 2007;41:5747–55.
- Bradley PM, Chapelle FH. Factors affecting microbial 2,4,6-Trinitrotoluene mineralization in contaminated soil. Environ Sci Technol 1995;29:802–6.
- Bromley AM. Weather observations, Wright Valley, Antarctica. New Zealand Meteorological Service; 1985.
- Christner BC, Mikucki JA, Foreman CM, Denson J, Priscu JC. Glacial ice cores: a model system for developing extraterrestrial decontamination protocols. Icarus 2005;74:572–84.

- Cowan DA, Tow LA. Endangered Antarctic environments. *Annu Rev Microbiol* 2004;58:649–90. doi:10.1146/annurev.micro.57.030502.090811.
- DESC (Defense Energy Support Center). Turbine fuel, aviation JP8/AN8 (Deep Freeze); 2005.
- Edwards T. Advancements in gas turbine fuels from 1943 to 2005, vol. 129. *J. of Engineering for Gas Turbines and Power-Transactions of the Asme*; 2007. p. 13–20.
- Foreman CM, Sattler B, Mikucki JA, Porazinska DL, Priscu JC. Metabolic activity and diversity of cryoconites in the Taylor Valley, Antarctica. *J Geophys Res* 2007;112:G04S32. doi:10.1029/2006JG000358.
- Fritsen CH, Priscu JC. Cyanobacterial assemblages in permanent ice covers on Antarctic lakes: distribution growth rate, and temperature response of photosynthesis. *J Phycol* 1998;34:587–97.
- Gore DB, Revill AT, Guille D. Petroleum hydrocarbons ten years after spillage at a helipad in Bunge Hills, East Antarctica. *Antarct Sci* 1999;11:427–9.
- Henderson RA, Prebble WM, Hoare RA, Popplewell KB, House DA, Wilson AT. An ablation rate for Lake Fryxell, Victoria Land, Antarctica. *J Glaciol* 1965;6:129–33.
- Hendy CH. The role of polar lake ice as a filter for glacial lacustrine sediments. *Geogr Ann A* 2000;82A:271–4.
- Hendy CH, Sadler AJ, Denton GH, Hall BL. Proglacial lake—ice conveyors: a new mechanism for deposition of drift in polar environments. *Geogr Ann A* 2000;82:249–70.
- Jepsen SM, Adams EE, Priscu JC. Fuel movement along grain boundaries in ice. *Cold Reg Sci Technol* 2006;45:158–65.
- Kennicutt II MC, McDonald TJ, Denoux GJ, McDonald SJ. Hydrocarbon contamination on the Antarctic Peninsula I. Arthur Harbor-subtidal sediments. *Mar Pollut Bull* 1992;10:499–506.
- Langbehn A, Steinhart F. Biodegradation studies of hydrocarbons in soils by analyzing metabolites formed. *Chemosphere* 1995;30:855–68.
- Leahy JG, Colwell RR. Microbial-degradation of hydrocarbons in the environment. *Microbiol Rev* 1990;54:305–15.
- Lyons WB, Nezat CA, Welch KA, Kottmeier ST, Doran PT. Fossil fuel burning in Taylor Valley, southern Victoria Land, Antarctica: estimating the role of scientific activities on carbon and nitrogen reservoirs and fluxes. *Environ Sci Technol* 2000;34:1659–62.
- Lyons WB, Laybourn-Parry J, Welch KA, Priscu JC. Antarctic lake systems and climate change. In: Bergstrom DM, Convey P, Huiskes AHL, editors. *Trends in Antarctic terrestrial and limnetic ecosystems: Antarctica as a global indicator*. Dordrecht: Springer; 2006.
- Mackay D, Shiu WY, Ma KC. *Handbook of physical-chemical properties and environmental fate for organic chemicals, vol. 2, polynuclear aromatic hydrocarbons, polychlorinated dioxins and debenzofurans*. London, UK: Lewis Publisher; 1992.
- Margesin R, Schinner F. Biological decontamination of oil spills in cold environments. *J Chem Technol and Biot* 1999;74:381–9.
- Mcknight DM, Niyogi DK, Alger AS, Bomblies A, Conovitz PA. Dry valley streams in Antarctica: ecosystems waiting for water. *Bioscience* 1999;49:985–95.
- MIL-DTL-83133E, 1999. Turbine fuels, aviation, kerosene type NATO F-34 (JP-8) NATO F-35 and JP-8+100.
- MIL-PRF-5624S, 1996. Turbine fuel, aviation, grades JP-4, JP-5, and JP-5/JP-8 ST.
- Parker BC, Simmons Jr GM, Wharton Jr RA, Seaburg KG. Removal of organic and inorganic matter from Antarctic lakes by aerial escape of blue-green algal mats. *J Phycol* 1982;18:72–8.
- Pawliszyn J. *RSC Chromatography Monographs*. In: Smith RM, editor. *Applications of solid phase microextraction* Cambridge U.K.: Royal Society of Chemistry; 1999. p. 655.
- Prince RC, Garrett RM, Bare RE, Grossman MJ, Townsend T, Sufilita JM, et al. The roles of photooxidation and biodegradation in long-term weathering of crude and heavy fuel oils. *Spill Sci Technol Bull* 2003;8:145–56.
- Priscu JC. Life in the valley of the dead. *Bioscience* 1999;49:12,9.
- Priscu JC, Fritsen CH, Adams EE, Giovannoni SJ, Paerl HW, McKay CP, et al. Perennial Antarctic lake ice: an oasis for life in a polar desert. *Sci* 1998;280:2095–8.
- Priscu JC, Foreman CM. *Lakes of Antarctica*. Encyclopedia of Inland Waters. Elsevier Press; in press.
- Roberts EC, Laybourn-Parry J, McKnight DM, Novarinos G. Stratification and dynamics of microbial loop communities in Lake Fryxell, Antarctica. *Freshw. Biol* 2000;44:649–61.
- Saul DJ, Aislabie JM, Brown CE, Harris L, Foght JM. Hydrocarbon contamination changes the bacterial diversity of soil from around Scott Base, Antarctica. *FEMS Microbiol Ecol* 2005;53:141–55.
- Snape I, Harvey PMA, Ferguson SH, Rayner JL, Revill AT. Investigation of evaporation and biodegradation of fuel spills in Antarctica-I. A chemical approach using GC-FID. *Chemosphere* 2005;61:1485–94.
- Treonis AM, Wall DH, Virginia RA. Invertebrate biodiversity in Antarctic Dry Valley soils and sediments. *Ecosystems* 1999;2:482–92.
- Vincent WF. *Environmental management of a cold desert ecosystem: the McMurdo Dry Valleys*. Desert Research Institute; 1996. p. 57.
- Virginia RA, Wall DH. How soils structure communities in the Antarctic Dry Valleys. *BioScience* 1999;49:973–83.
- Wang ZD, Fingas M, Blenkinsopp S, Sergy G, Landriault M, Sigouin L, et al. Comparison of oil composition changes due to biodegradation and physical weathering in different oils. *J Chromatogr A* 1998;809:89–107.
- Wharton RA, Doran PT. *McMurdo Dry Valle Lakes: impacts of research activities*. Chicago: University of Illinois at Chicago; 1999. p. 54.
- Zürcher F, Thüer M. Rapid weathering processes of fuel oil in natural waters. *Environ Sci Technol* 1978;12:838–43.